Room-temperature lasing at 1.82 μm of GaInSb/AlGaSb quantum wells grown on GaAs substrates using an interfacial misfit array

J. Tatebayashi,[a] A. Jallipalli, M. N. Kutty, S. H. Huang, G. Balakrishnan, L. R. Dawson, and D. L. Huffaker[b]
Center for High Technology Materials, University of New Mexico, 1313 Goddard SE, Albuquerque, New Mexico 87106, USA

(Received 13 July 2007; accepted 10 September 2007; published online 1 October 2007)

The authors report the device characteristics of GaInSb/AlGaSb quantum well (QW) lasers monolithically grown on GaAs substrates. The 7.8% lattice mismatch between GaAs substrates and GaSb buffer layers can be completely accommodated by using an interfacial misfit (IMF) array. Room-temperature lasing operation is obtained from a 1.25-mm-long device containing six-layer $Ga_{0.9}In_{0.1}Sb/Al_{0.35}Ga_{0.65}Sb$ QWs at 1.816 μm with a threshold current density of 1.265 kA/cm^2. The observed characteristic temperature and temperature coefficient are 110 K and 9.7 Å/K, respectively. This IMF technique will enable a wide range of lasing wavelengths from near-infrared to midwavelength-infrared regimes on a GaAs platform. © *2007 American Institute of Physics*. [DOI: 10.1063/1.2793186]

GaAs-based innovative material systems have recently attracted practical interest for the application to optical devices including vertical-cavity surface-emitting lasers (VCSELs) which can cover the near-infrared (NIR) regimes. Several approaches to realize longer-wavelength emission on GaAs substrates have been reported including GaInNAs(Sb)-based quantum well[1–4] (QW) and GaIn(N)As-based quantum dots.[5,6] Continuous-wave lasing at 1.55 μm from GaInNAsSb QW lasers has been obtained at room temperature (RT).[4] However, substantial deterioration of the crystal quality due to lattice mismatch and strain might hinder the extension of the lasing wavelength toward >1.6 μm on a GaAs platform.

A Sb-based material system is an attractive candidate for several applications to medical diagnostics or military scene projection that require emitters or detectors operating at the NIR (>1.55 μm)[7–11] or the midwavelength-IR (MWIR) regime (2–5 μm).[12–19] Above all, high performance lasers with low threshold current density (J_{th}), high modal gain, high characteristics temperature (T_0), or high output power have been recently demonstrated.[16–19] These characteristics of Sb-based lasers emitting in the NIR regime have become almost comparable to those of the InP-based lasers. However, commercialization of Sb-based devices would be enhanced by developing the devices on an established material platform such as GaAs substrates, which might be able to circumvent the challenges associated with the Sb-platform to realize the MWIR photonic devices with a low-cost performance. In addition, the use of *n*-type GaAs substrates instead of GaSb might overcome the substantial problem of immature contact system to *n*-type GaSb. So far, a scheme to grow compositionally graded metamorphic buffers has been attempted to realize Sb-based devices on GaAs substrates.[20]

An interfacial misfit (IMF) growth mode offers a method to grow Sb-based materials on a GaAs platform without using thick metamorphic buffers to relieve the 7.8% lattice mismatch between GaAs and GaSb.[21,22] By monolithically integrating Sb-based actives onto GaAs substrates, lasers emitting in an extremely wide range of not only the visible or NIR but also the MWIR regimes can be obtained. This IMF technology has also led to the demonstration of optically pumped GaSb/AlGaSb VCSELs grown on Si substrates[23] and an electrically injected GaSb/AlGaSb vertical light-emitting diodes and lasers grown on GaAs substrates.[24,25] Work has also been conducted on the atomic modeling and the material characterization of the IMF interface.[22]

In this study, Sb-based laser structures are monolithically grown on (100) *n*-GaAs substrates by solid-state molecular beam epitaxy. Figure 1(a) shows a schematic illustration of the fabricated laser structure. The growth is initiated with a 100 nm GaAs buffer layer grown at 580 °C followed by the IMF formation and 5 nm of *n*-doped GaSb growth. The IMF array can be observed from cross-sectional transmission electron microscope (TEM) images, as shown in Fig. 1(b), at the interface between GaAs and GaSb. The space between the misfit dislocations of ≅56 Å [Fig. 1(c)] is expected from the $\Delta a_0/a_0=7.8\%$.[21,22] A conventional growth technique for Sb-based devices is performed after deposition of thin GaSb, followed by a 2.3 μm *n*-$Al_{0.45}Ga_{0.55}Sb$ clad, an active 1.5 μm *p*-$Al_{0.45}Ga_{0.55}Sb$ clad, and a 50 nm p^+-GaSb contact layer with a doping density of $2\times10^{19}/cm^3$. The growth

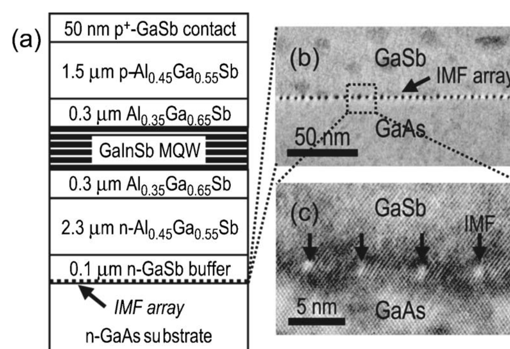

FIG. 1. Schematic illustration of the fabricated six-layer $Ga_{0.9}In_{0.1}Sb/Al_{0.35}Ga_{0.65}Sb$ QW laser structure. (b) and (c) are cross-sectional TEM images of the IMF array between GaAs and GaSb.

[a]Electronic mail: tatebaya@chtm.unm.edu
[b]Electronic mail: huffaker@chtm.unm.edu

 © 2007 American Institute of Physics
Downloaded 01 Oct 2007 to 64.106.37.204. Redistribution subject to AIP license or copyright, see http://apl.aip.org/apl/copyright.jsp

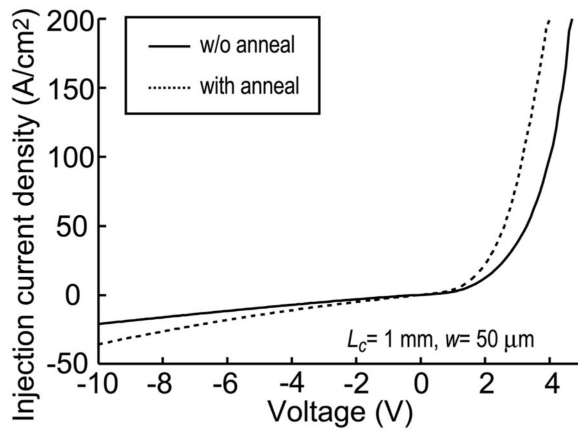

FIG. 2. *I-V* characteristics of the fabricated lasers with and without annealing for metal contact.

temperatures of all the layers except for GaAs buffer are 510 °C. Si and Be are used as *n*- and *p*-type doping materials, respectively. A low doping density of $5\times10^{17}/\text{cm}^3$ is used for *n*- or *p*-$Al_{0.45}Ga_{0.55}Sb$ close to the waveguide and then increased to $1\times10^{18}/\text{cm}^3$ for the rest of $Al_{0.45}Ga_{0.55}Sb$ clad layer. The active layer consists of six-layer 17 nm $Ga_{0.9}In_{0.1}Sb$ QWs separated by 20 nm $Al_{0.35}Ga_{0.65}Sb$ barriers, and is sandwiched by 300 nm $Al_{0.35}Ga_{0.65}Sb$ separated confinement heterostructures. Broad area edge emitters (25-μm-wide stripe) are fabricated by a conventional top-bottom device processing with as-cleaved facets on both sides. This process involves a Ti/Pt/Au evaporation for p^+-GaSb top contact, an inductively coupled plasma reactive ion etching of the *p* clad, lapping of the GaAs substrate to ~150 μm, and a Ge/Au/Ni/Au evaporation for *n*-GaAs bottom contact.

Figure 2 shows the current-voltage (*I-V*) characteristics of the fabricated lasers with and without annealing processes for an Ohmic contact, indicating high diode turn on voltages of 2.2 and 2.9 V, respectively, even though the expected turn-on voltage is ≅1 V. This difference of the turn-on voltage between the devices with and without annealing processes is likely due to a contact potential (≅0.7 V) resulting from an unannealed Ge/Au/Ni/Au contact to the *n*-GaAs substrate. Possible contributions to the excess voltage even after annealing process include a potential drop at the GaAs/GaSb IMF interface predicted to be ≅0.7 V.[24] According to modeling, the potential drop at the IMF can be improved by delta doping the interface to compensate the acceptorlike dangling bonds.[21] However, current injection across the IMF can be avoided completely by using a top-top contacting scheme. In reverse bias, a recombination current of 35 A/cm^2 (annealed device) and 21 A/cm^2 (unannealed device) is observed at −10 V. This comparatively large recombination current is likely due to threading dislocations that result from the unoptimized and imperfect IMF array. A larger recombination current for the annealed device may result from the reduced contact resistance or an increased threading dislocation by an annealing process.

Measurements of laser characteristics are performed on a temperature-controlled stage with *n*-side down under pulsed operations with a repetition rate of 0.5 kHz (2 ms period) and duty cycle ranging from 0.05% to 4%. Peak output power-current (*L-I*) characteristics and electroluminescence (EL) spectra are collected using a spectrometer, InGaAs IR

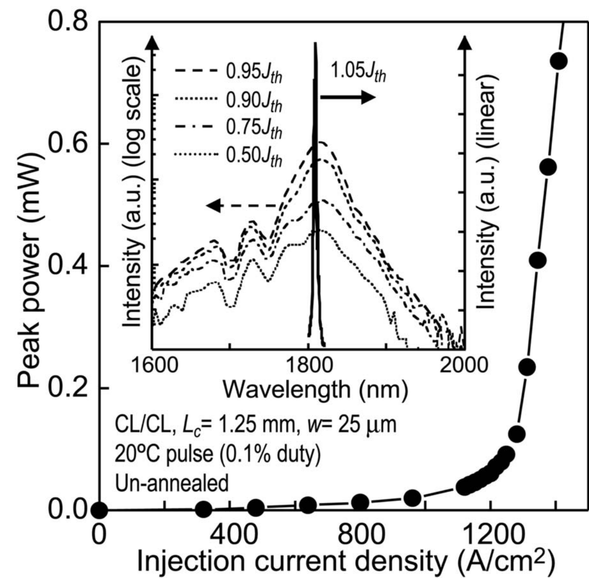

FIG. 3. *L-I* characteristics of six-layer $Ga_{0.9}In_{0.1}Sb/Al_{0.35}Ga_{0.65}Sb$ QW lasers with L_c=1.25 mm at 20 °C under a pulsed condition (0.1% duty cycle). Inset is EL spectra with different J ranging from $0.5J_{th}$ to $1.05J_{th}$.

detector, and an integrating sphere. *L-I* curve in Fig. 3 shows lasing operation with a threshold current density (J_{th}) of 1.265 kA/cm^2 at a stage temperature of 20 °C (0.1% duty cycle). An output peak power of ≅1 mW is obtained at an injection current density (J) of 1.5 kA/cm^2. An inset of Fig. 3 shows EL spectra at various J ranging from $0.5J_{th}$ to $1.05J_{th}$ with a cavity length (L_c) of 1.25 mm. The EL emission from the fabricated device emerges at a peak wavelength of ≅1.82 μm and lasing peak is observed at 1.816 μm. We have already demonstrated RT lasing at 1.62 μm from six-layer $GaSb/Al_{0.35}Ga_{0.65}Sb$ QWs with J_{th} =3 kA/cm^2, as reported in Ref. 25, indicating that the lasing wavelength (λ_{pk}) can be altered by changing the composition of the QW matrices. Improvement of J_{th} is due to the increased gain caused by the compressive strain between GaInSb and AlGaSb materials by incorporating indium into QW matrices.

Figure 4(a) plots the J_{th} and λ_{pk} near the threshold of a 1.25-mm-long device versus a stage temperature under the pulsed operation (0.1% duty cycle) with different stage temperatures from −10 to 35 °C. A calculated value of T_0 is 110 K over the stage temperature ranging from −10 to 35 °C. A value of J_{th} can be expressed as $J_{th} = qV(AN+BN^2+CN^3)/\eta_i$, where q is an elementary electric charge, V is an active region volume, η_i is an internal quantum efficiency, N is a carrier density, and A, B, and C are coefficients. A value of comparatively high T_0 is due to the large monomolecular recombination coefficient of A which does not vary much with the stage temperature, resulting in the relatively insensitive J_{th} against the stage temperature. A temperature coefficient, defined by the shift of λ_{pk} against the stage temperature, is determined to be 9.7 Å/K, which is somewhat larger than that reported by other group for the same GaSb-based materials.[7] Figure 4(b) plots the λ_{pk} with different duty cycles ranging from 0.05% to 4%. A redshift of the λ_{pk} is observed by increasing the duty cycle, and the λ_{pk} shifts toward 8 nm longer at a duty cycle of 4%. The observed 8 nm redshift might be caused by a heat effect from the potential drop at the IMF interface lying much closer to

Downloaded 01 Oct 2007 to 64.106.37.204. Redistribution subject to AIP license or copyright, see http://apl.aip.org/apl/copyright.jsp

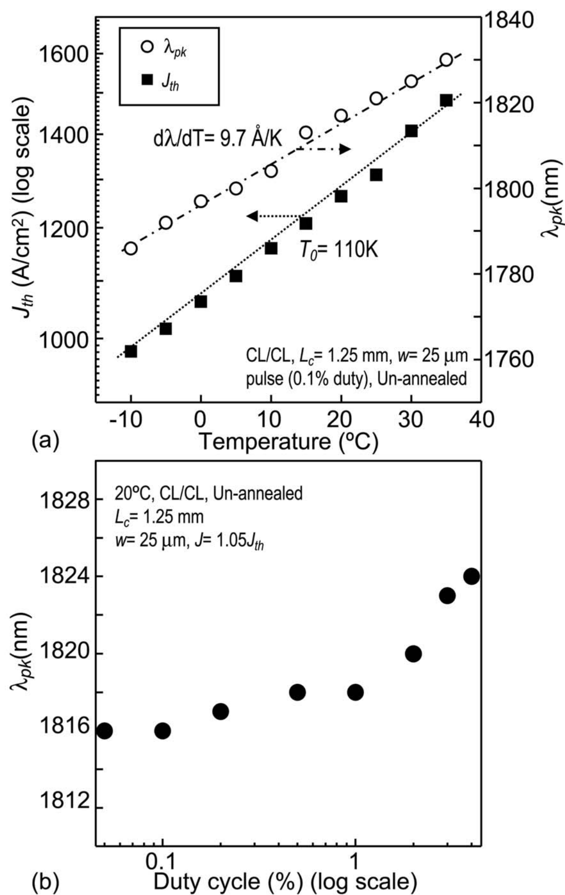

FIG. 4. (a) Temperature dependence of the J_{th} and λ_{pk} under a pulsed condition (0.1% duty cycle). (b) λ_{pk} vs duty cycles ranging from 0.05% to 4%.

the active region than the temperature-controlled stage, or a lower thermal conductivity of GaSb-based materials than that of GaAs-based materials. Further investigation of the heat effect will be required including the comparison to the device with top-top contact processing.

In summary, we report the device characteristics of GaInSb/AlGaSb QW lasers monolithically grown on GaAs substrates by using the IMF array. The IMF interface can completely relieve the strain between GaAs substrate and GaSb buffer layer without using thick metamorphic buffers. RT lasing is obtained from a 1.25-mm-long device containing six layers $Ga_{0.9}In_{0.1}Sb$ QWs at 1.816 μm with J_{th} $=1.265$ kA/cm^2. The observed T_0 and temperature coefficient are 110 K and 9.7 Å/K, respectively. *I-V* characteristics indicate a high diode turn on of 2.9 V for unannealed devices. Possible contribution of the excess voltage includes a predicted 0.7 V potential drop at the GaAs/GaSb IMF interface. Further growth optimization will be required for reducing the threading dislocation density caused by the unoptimized and imperfect IMF array and alleviating the potential drop at the IMF interface. However, this IMF technique can enable a wide range of the lasing wavelength from the visible to NIR or even MWIR regimes on a GaAs platform.

This work is supported by the Defense Advanced Research Projects Agency, University Photonic Research Centers (Dr. Jagdeep Shah), and the Air Force Office of Scientific Research. The authors would like to thank A. Albrecht for their support of laser characterization.

[1] M. Kondow, K. Uomi, A. Niwa, T. Kitatani, S. Watahiki, and Y. Yazawa, Jpn. J. Appl. Phys., Part 1 **35**, 1273 (1996).
[2] X. Yang, M. J. Jurkovic, J. B. Heroux, and W. I. Wang, Appl. Phys. Lett. **75**, 178 (1999).
[3] W. Ha, V. Gambin, S. Bank, M. Wistey, H. Yuen, S. Kim, and J. S. Harris, Jr., IEEE J. Quantum Electron. **38**, 1260 (2002).
[4] S. R. Bank, H. P. Bae, H. B. Yuen, M. A. Wistey, L. L. Goddard, and J. S. Harris, Jr., Electron. Lett. **42**, 156 (2006).
[5] M. Sopanen, H. P. Xin, and C. W. Tu, Appl. Phys. Lett. **76**, 994 (2000).
[6] J. Tatebayashi, M. Nishioka, and Y. Arakawa, Appl. Phys. Lett. **78**, 3469 (2001).
[7] G. Motosugi and T. Kagawa, Jpn. J. Appl. Phys., Part 1 **19**, 2303 (1980).
[8] Y. Ohmori, S. Tarucha, Y. Horikoshi, and H. Okamoto, Jpn. J. Appl. Phys., Part 2 **23**, L94 (1984).
[9] H. K. Choi, G. W. Turner, and S. J. Eglash, IEEE Photonics Technol. Lett. **6**, 7 (1994).
[10] G. Almuneau, F. Genty, A. Wilk, P. Grech, A. Joullié, and L. Chusseau, Semicond. Sci. Technol. **14**, 89 (1999).
[11] R. Werner, T. Bleuel, J. Hofmann, M. Brockhaus, and A. Forchel, IEEE Photonics Technol. Lett. **12**, 966 (2000).
[12] T. H. Chiu, W. T. Tsang, J. A. Ditzenberger, and J. P. van der Ziel, Appl. Phys. Lett. **49**, 1051 (1986).
[13] D. Z. Garbuzov, R. U. Martinelli, H. Lee, P. K. York, R. J. Menna, J. C. Connolly, and S. Y. Narayan, Appl. Phys. Lett. **69**, 2006 (1996).
[14] G. W. Turner, H. K. Choi, and M. J. Manfra, Appl. Phys. Lett. **72**, 876 (1998).
[15] C. Mermelstein, S. Simanowski, M. Mayer, R. Kiefer, J. Schmitz, M. Walther, and J. Wagner, Appl. Phys. Lett. **77**, 1581 (2000).
[16] J. G. Kim, L. Shterengas, R. U. Martinelli, G. L. Belenky, D. Z. Garbuzov, and W. K. Chan, Appl. Phys. Lett. **81**, 3146 (2002).
[17] M. Garcia, A. Salhi, A. Pérona, Y. Rouillard, C. Sirtori, X. Marcadet, and C. Alibert, IEEE Photonics Technol. Lett. **16**, 1253 (2004).
[18] M. Grau, C. Lin, O. Dier, C. Lauer, and M.-C. Amann, Appl. Phys. Lett. **87**, 241104 (2005).
[19] L. Shterengas, G. Belenky, M. V. Kisin, and D. Donetsky, Appl. Phys. Lett. **90**, 011119 (2007).
[20] Y.-C. Xin, L. G. Vaughn, L. R. Dawson, A. Stintz, Y. Lin, L. F. Lester, and D. L. Huffaker, J. Appl. Phys. **94**, 2133 (2003).
[21] S. H. Huang, G. Balakrishnan, A. Khoshakhlagh, A. Jallipalli, L. R. Dawson, and D. L. Huffaker, Appl. Phys. Lett. **88**, 131911 (2006).
[22] A. Jallipalli, G. Balakrishnan, S. H. Huang, A. Khoshakhlagh, L. R. Dawson, and D. L. Huffaker, J. Cryst. Growth **303**, 449 (2007).
[23] G. Balakrishnan, A. Jallipalli, P. Rotella, S. H. Huang, A. Khoshakhlagh, A. Amtout, S. Krishna, L. R. Dawson, and D. L. Huffaker, IEEE J. Sel. Top. Quantum Electron. **12**, 1636 (2006).
[24] M. Mehta, G. Balakrishnan, S. H. Huang, A. Khoshakhlagh, A. Jallipalli, P. Patel, M. N. Kutty, L. R. Dawson, and D. L. Huffaker, Appl. Phys. Lett. **89**, 211110 (2006).
[25] M. Mehta, G. Balakrishnan, A. Jallipalli, M. N. Kutty, L. R. Dawson, and D. L. Huffaker, *Proceedings of the 65th Device Research Conference*, 2007, p. 193

Downloaded 01 Oct 2007 to 64.106.37.204. Redistribution subject to AIP license or copyright, see http://apl.aip.org/apl/copyright.jsp